Fluorescent Liposome Flow Markers for Microscale Particle-Image Velocimetry

3 AUTHORS, INCLUDING:

Anup K Singh
Sandia National Laboratories
150 PUBLICATIONS **3,805** CITATIONS

SEE PROFILE

Eric B. Cummings
LabSmith, Inc
76 PUBLICATIONS **1,649** CITATIONS

SEE PROFILE

Fluorescent Liposome Flow Markers for Microscale Particle-Image Velocimetry

Anup K. Singh,* Eric B. Cummings, and Daniel J. Throckmorton

Sandia National Laboratories, P.O. Box 969, Livermore, California 94551-0969

Unilamellar liposomes carrying both encapsulated and surface-immobilized fluorophores have been synthesized as novel fluorescent markers to image flow profiles in microfabricated structures. The unilamellar liposomes were made with phospholipids and cholesterol by extrusion through a polycarbonate membrane. They contained carboxyfluorescein in the aqueous core and fluorescein-labeled lipids in the bilayer to render them both a surface and volume fluorescer, maximizing their fluorescence intensity. The lipid composition was chosen to impart a net negative charge to liposomes to minimize self-aggregation as well as interaction with negatively charged glass surfaces of the channels. These liposomes were monodisperse (mean diameter 283 nm), neutrally buoyant, and hydrophilic and exhibited no adsorption on glass surfaces. Unlike polystyrene spheres, they were readily broken up by surfactants, thereby allowing for easy and complete removal from microfluidic channels. The fluorescent liposomes were used to investigate pressure-driven flow in an offset cross intersection in a microfluidic chip and provided images with excellent signal-to-noise ratio. A novel computational scheme that is particularly suitable for analyzing particle-image velocimetry data in micrometer-scale flow channels was employed to analyze the images. These liposomes are easily synthesized and can be custom-made for various applications to offer a broad range of surface and volume characteristics such as charge, size, and surface chemistry.

Microfabricated chemical/biochemical analysis and synthesis systems have attracted a significant amount of research and commercial interest, especially in biological and medical applications.[1,2] In pursuit of speed, portability, high throughput, and reduced costs, demand is being placed on miniaturization of existing analysis systems as well as development of microsystems that rely on techniques enabled at the micrometer scale. While a number of microsystems rely on fluid transport by using electrical or hydrostatic means, relatively few studies have been undertaken to understand performance-limiting phenomena in practical microfluidic systems. For example, flow in microstructures can be strongly influenced by surface tension-related effects as well as seemingly minor architectural and surface defects. Moreover, the geometrical and electrical flow control that is possible at the

micrometer scale should enable the design of novel and extremely high-performance chemical assays using microfabricated structures. A precise understanding of flow and transport in these systems is crucial to realizing the benefits of this control. While progress has been made in microfluidic simulation[3] and theory,[4,5] in situ imaging experiments are the only reliable methods of diagnosing the sources of dispersion in simple as well as complex systems that can have multiple intersecting channels and heterogeneous fluids and surfaces.

A number of experimental approaches such as imaging using fluorophores[6,7] and caged dyes[8] have been explored for examining flow fields in capillaries. Particle-image velocimetry (PIV), a standard macroscale flow-diagnostic technique,[9] has recently been applied to the study of microflows.[10−12] In this technique, particles suspended in the fluid are imaged onto a recording device, typically a CCD camera. By comparing the location of the particle images in frames taken a suitable time interval apart, the motion of the fluid may be inferred with good accuracy and spatial resolution. In order for the particles to trace the flow faithfully without affecting it, they must be much smaller than the smallest geometrical flow features. For typical microsystems, this constrains particles to the submicrometer scale. Because of the small size of the particles and the presence in microsystems of bounding surfaces that scatter and reflect light, microfluidic PIV is typically performed by imaging the fluorescence of dye-tagged particles. Commercially available fluorescent latex microspheres provide an inexpensive and convenient flow marker for PIV. However, these microspheres typically fluoresce only on the surface or fluoresce only weakly through the volume because of the quenching effects in the solid phase. The relatively weak fluorescence of these spheres limits the signal-to-noise ratio of the particle images taken using uncooled CCDs and typical epifluorescence illumination sources. Another drawback of latex particles is that they are

(1) Sanders, G. H. W.; Manz, A. *Trends Anal. Chem.* **2000,** *19,* 364−378.
(2) Figeys, D.; Pinto, D. *Anal. Chem.* **2000,** *72,* 330A−335A.

(3) Ermakov, S. V.; Jacobson, S. C.; Ramsey, J. M. *Anal. Chem.* **1998,** *70,* 4494−4504.
(4) Cummings, E. B.; Griffiths, S. K.; Nilson, R. H.; Paul, P. H. *Anal. Chem.* **2000,** *72,* 2526−2532.
(5) Rathore, A. S.; Horvath, C. *J. Chromatogr., A* **1997,** *781,* 185−195.
(6) Taylor, J. A.; Yeung, E. S. *Anal. Chem.* **1993,** *65,* 2928−2932.
(7) Kuhr, W. G.; Licklider L.; Amankwa, L. *Anal. Chem.* **1993,** *65,* 277−282.
(8) Paul, P. H.; Garguilo, M. G.; Rakestraw, D. J. *Anal. Chem.* **1998,** *70,* 2459−2467.
(9) Keane, R. D.; Adrian, R. J.; Zhang, Y. *Meas. Sci. Technol.* **1995,** *6,* 754.
(10) Santiago, J. G.; Wereley, S. T.; Meinhart, C. D.; Beebe, D. J.; Adrian, R. *Exp. Fluids* **1998,** *25,* 316−319.
(11) Meinhart, C. D.; Wereley, S. T.; Santiago, J. G. *Exp. Fluids* **1999,** *27,* 414−419.
(12) Meinhart, C. D.; Wereley, S. T.; Gray, M. H. B. *Meas. Sci. Technol.* **2000,** *11,* 809−814.
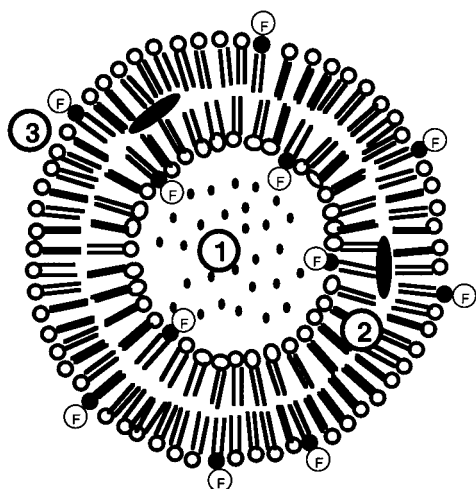
Figure 1. Cross section of a unilamellar liposome. Water-soluble molecules can be entrapped in the aqueous core (region 1) or linked to the outer surface (region 3); hydrophobic molecules can be entrapped in the bilayer (region 2). Fluorescent liposomes made for PIV contain both encapsulated (in region 1) and surface-attached fluoroprophores (labeled F).

Figure 2. Schematic of the inverted epifluorescence microscope, the microfluidic circuit, and the test fixture used in the PIV experiments using liposomes. The fixture contains a vacuum chuck for reliably and reversibly sealing 16 fluidic ports to the microfuidic circuit.

generally hydrophobic because the base polymer is polystyrene. While various modifications are often made to increase the charge and hydrophilicity of the latex particles, the particles always retain some hydrophobic characteristics.[13] This can potentially lead to the aggregation of particles, nonspecific adsorption of hydrophobic solutes on the particle surface, and adhesion of latex particles to microchannel surfaces.

We present fluorescent liposomes as an alternative to fluorescent latex microspheres for imaging flows in microchannels. Liposomes can be efficient surface *and* volume fluorescers as dyes can be encapsulated in the aqueous core as well as immobilized in the lipid bilayer (by using fluorophore-labeled lipids). They can be made with relatively low variation in size and electrophoretic mobility and are neutrally buoyant (to minimize sedimentation) in aqueous solutions. Furthermore, they afford the researcher an exceptional ability to modify the surface and volume properties to suit a specific application. Liposomes can be made out of thousands of natural or synthetic lipids that are commercially available. Depending on the choice of lipids, they can be made cationic, anionic, or neutral and can have headgroups containing functional moieties such as amines, carboxyls, sugars, or sulfhydryls. Typically liposomes are made to carry a few charges on the surface to minimize aggregation. Unlike latex particles, liposome surfaces are very hydrophilic, thereby reducing aggregation and hydrophobic interactions with other molecules and surfaces. Stable unilamellar liposomes can be prepared in diameters ranging from 40 nm to 0.5 μm; liposomes larger than 1 μm tend to be unstable and aggregate over time.[14] Liposomes are excellent storage and delivery vehicles owing to their capacity to encapsulate a large number of small molecules in the core, in the bilayer, or on the surface (Figure 1). Hydrophilic molecules can be encapsulated in the core or attached to the outer surface and hydrophobic molecules can be embedded in the bilayer. This
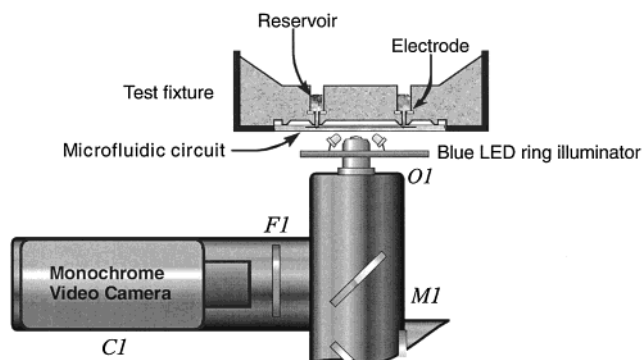
property has allowed them to be applied in a multitude of applications such as drug[15] and gene[16] delivery and immunodiagnostics.[17]

Finally, liposomes offer a practical advantage over latex particles as well; they are easier to clean from microfluidic structures after use. Liposomes can rapidly be broken into monomers by organic solvents or into micelles by detergents, making their complete removal from microfabricated structures quite convenient and fast. Latex particles, on the other hand, if dried out or trapped in stagnant regions can require relatively long time and extensive washing for complete removal.

EXPERIMENTAL SECTION

Imaging Apparatus. The experimental apparatus is shown schematically in Figure 2. The microflows are imaged by an LED-illuminated, inverted, video epifluorescence microscope. A ring of 24 blue LEDs (Nichia, NSPB300A) flood illuminates the sample with light having a peak wavelength of 470 nm. A 10× microscope objective (O1) images a 520-μm × 390-μm region of the circuit onto camera C1. Dichroic mirror M1 reflects fluorescence in the wavelength range below ∼550 nm into an emission filter F1, which further limits the signal wavelength range to 500−530 nm. The filtered signal falls on a video-rate monochromatic $^{1}/_{2}$-in. CCD camera (Cohu 4910, C1).

PIV. Experiments were conducted on microflows in a microfluidic circuit consisting of patterned channels isotropically etched ∼10 μm deep in glass with a thermally bonded glass cover. The geometry used for imaging flow was an offset cross intersection consisting of two tees (Figure 4a). The microfluidic circuit is reversibly sealed to a test fixture via a vacuum chuck. This fixture provides 16 open, 1-mL fluid reservoirs. Ports drilled in the cover slip align with reservoirs in the test fixture made of poly-(dimethylsiloxane) (PDMS). Connections between the test circuit and fixture were secured by drawing a vacuum in a cavity between the test circuit and fixture that is isolated from the reservoirs.

(13) Product Information Sheet on FluoSpheres Fluorescent Microspheres, Molecular Probes, Eugene, OR, 1997.
(14) New, R. R. C. *Liposomes: A Practical Approach*; IRL Press: Oxford, 1990.

(15) Gregoriadis, G. *Liposome Technology: Targeted Drug Delivery and Biological Interaction*; CRC Press: Boca Raton, FL, 1984.
(16) Lasic, D. D. *Liposomes in Gene Delivery*; CRC Press: Boca Raton, FL, 1997.
(17) (a) Singh, A. K.; Schoeniger J. S.; Carbonell, R. G. *Biosensors and Their Applications*; Yang, V. C., Ngo, T. T., Eds.: Kluwer Academic/Plenum Publishing: New York, 1999; pp 131−145. (b) Singh, A. K.; Carbonell, R. G. *Nonmedical Applications of Liposomes*; Lasic, D. L., Barenholz, Y., Eds.; CRC Press: Boca Raton, FL, 1995; pp 209−228.

This removable connection allowed the use of cleaning chemicals on the test circuit that are not compatible with the test fixture.

Thirty 8-bit $\times$ 640- $\times$ 480-pixel images from the camera were recorded directly to disk per second. Each experimental run consisted of 1000 images (33 s, $\sim$300 MB). These images were processed using an iterative, adaptive-gridding cross-correlation algorithm (described elsewhere[18]) that extracted detailed velocity measurements shown in the following section. Briefly, velocity measurements are obtained by subdividing pairs of images into typically 32- $\times$ 32-pixel subimages. Each subimage from the first image is correlated via fast Fourier transform techniques with the corresponding subimage from the second image in the pair. The location of the correlation peak provides a statistical estimate of the Cartesian displacement between the particle subimages that maximizes their similarity. Hence, a measure of the mean particle displacement between each subimage is obtained. The initial measurement of the displacement is refined inidividually for each subimage by one or all of the following procedures: (1) subdividing the subimages to half their original size, (2) choosing the number of frames in the video to skip between correlation pairs so the particle displacement between them is approximately equal to the subimage size, and (3) shifting the location of the subimages in the image pairs to follow the mean particle displacement.

The images are again correlated with these grid optimizations, producing improved estimates of the velocities. This refinement procedure iterates to convergence. The final subimage size is selected to minimize errors from flow gradients and finite particle statistics. The measurements presented here use a final subimage size of 8 $\times$ 8 pixels or $\sim$6-μm spatial resolution. Velocity measurements are extracted from the correlations by the use of an optimal nonlinear filter that accounts for finite particle Peclet number effects, velocity gradients in the unresolved (depth) direction, and statistical variation of particle electrophoretic mobility (for electrically driven flows).

Preparation of Fluorescent Liposomes. Unilamellar liposomes were prepared with composition of L-α-distearoylphosphatidylcholine) (DSPC)/cholesterol/L-α-dimyristoylphosphatidylethanolamine (DMPE)/N-fluorescein-5-thiocarbamoyl-1,2-dihexadecanoyl-sn-glycero-3-phosphoethanolamine (fluorescein-DHPE) in a mole ratio of 0.4:0.4:0.15:0.5 by the extrusion procedure.[19] Stock solutions typically at a concentration of 10 mg/mL of lipids were prepared in 9:1 chloroform$-$methanol (v/v). Mixtures of various lipids amounting to 10 μmol total were added to a round-bottomed flask. The flask was connected to a rotary evaporator and dried at 60 °C for 1.5 h to form a thin lipid film on the inside wall of the flask. The dried lipid layer was then hydrated in filtered and degassed 50 mM borate buffer, pH 9, containing 25 mM carboxyfluorescein for 1 h at 65 °C to form multilamellar liposomes. The multilamellar liposomes were sonicated briefly in a bath sonicator to reduce the average size of liposomes and then extruded through a 300-nm polycarbonate membrane in a pneumatic liposome extruder (Liposofast, Avestin, ON, Canada). Liposomes were extruded 31 times to ensure uniform size distribution. The resulting unilamellar liposome suspension was centrifuged for 20 min at 3000g to remove residual multilamellar liposomes and aggregated lipids. The unencapsulated carboxy-

fluoresein was separated from liposomes by size exclusion chromatography using a 15- $\times$ 1-cm gel filtration column equilibrated with 50 mM borate buffer at pH 9. Fractions (1 mL) were collected using a Spectra-Chrom fraction collector and were visually monitored for the presence of yellow color (due to fluorescein). Fractions containing liposomes were pooled and stored at 4 °C in dark.

Characterization of Liposomes. The hydrodynamic diameter of the liposome solution was estimated using a quasi-elastic light scattering (QELS) apparatus (Brookhaven Instruments, Holtsville, NY). In this technique, the time-dependent fluctuations of scattered light intensity are measured to determine the translational diffusion constant of a suspended particle, which in turn can be related to hydrodynamic radius using the Stokes$-$Einstein relation. Prior to the size measurement, the liposome solution was centrifuged at 3000 rpm for 20 min to precipitate any dust particles and aggregated lipids. Liposomes (50 μL) were diluted in 1.5 mL of freshly filtered buffer in a clean polypropylene cuvette and placed in the QELS apparatus. The measurement was performed at 90° scattering angle and the QELS data were analyzed using the constrained regularization (CONTIN) method to obtain a mean diameter and distribution.[20] The ζ potential of liposomes was measured by electrophoretic light scattering, which is based on the scattering of light from particles that move in a liquid under the influence of an applied electric field.[21] Liposomes were diluted in a 10 mM KCl solution for the measurement of ζ potential.

The number of lipids in a spherical unilamellar liposome, N_{tot}, can be estimated as[22]

$$N_{\text{tot}} = \pi/a_{\text{L}}[d^2 - (d - 2t)^2] \tag{1}$$

where t is the bilayer thickness, d is the hydrodynamic diameter, and a_{L} is the average headgroup area per lipid. The bilayer thickness was assumed to be 40 Å and a_{L} was calculated using values of 71, 41, and 19 Å^2 for phosphatidylcholine, phosphatidylamine, and cholesterol, respectively,[23] weighted by the appropriate mole fraction of each component. The headgroup area of fluorescein-DHPE was assumed to be the same as ethanolamine. This may cause some error in area calculation but since fluorescein-DHPE is present at a small concentration, the error should be relatively small. The value of a_{L} for liposomes was calculated as 44.8 Å^2/lipid. Liposome concentration in solution can be calculated by dividing the lipid concentration by N_{tot}. The number of fluorescein on the surface is 0.05N_{tot}/liposome. The number of encapsulated carboxyfluorescein molecules can be calculated knowing the internal volume of a liposome and the concentration of the dye.

RESULTS AND DISCUSSION

Markers or tracers to be used as flow markers in PIV should have the following characteristics: small size (so as not to perturb the flow), high fluorescence (for good S/N), near-zero buoyancy,

(18) Cummings, E. B. *Exp. Fluids* **2000**, *29*, 542$-$550.

(19) Mayer, L. D.; Hope, M. J.; Cullis, P. R. *Biochim. Biophys. Acta* **1986**, *858*, 161$-$168.

(20) Provencher, S. W. *Comput. Phys. Commun.* **1982**, *27*, 213$-$227.

(21) Weiner, B. B.; Tscharnuter, W. W.; Fairhurst, D. Product Literature, Brookhaven Instruments Corp., Holtsville, NY 11742.

(22) Singh, A. K.; Kilpatrick, P. K.; Carbonell, R. G. *Biotechnol. Prog.* **1996**, *12*, 272$-$280.

(23) Israelachvili, J. N.; Mitchell, D. J. *Biochim. Biophys. Acta* **1975**, *389*, 13$-$19.

Table 1. Characteristics of Fluorescent Liposomes Used as Flow Markers in PIV

concentration used for PIV	3×10^{-9} M (0.007 volume fraction)
hydrodynamic diameter	283 nm
ζ potential	-58 ± 1.7 mV
electrophoretic mobility	-4.3 $(\mu m/s)/(V/cm)$
no. of fluorescein in the bilayer	5.47×10^4
no. of fluorescein in the aqueous core	1.65×10^5
total no. of unquenched fluorescein equivalents	7.95×10^4

Figure 3. Size-distribution of the fluorescent liposomes as measured by quasi-elastic light scattering. The mean diameter of liposomes is 283 nm.

uniform size and surface properties, and stability. Furthermore, for reusable microfluidic systems, it is imperative that flow markers do not adhere to channel surfaces and can be flushed completely from the microfluidic system. We prepared fluorescent liposomes that meet all these criteria. The mean liposome diameter was 283 nm. Liposomes were used at a volume fraction of 0.007 to cause minimal alteration to the bulk flow. Liposomes contained ~165 000 carboxyfluorescein molecules in the core and 55 000 fluoresein-DHPE in the bilayer (Table 1). Incorporation of fluorophores in the core as well as the bilayer makes liposomes uniformly fluorescent over the entire particle volume. Moreover, in liposomes, all entrapped fluorophores are exposed to the buffer, maximizing their fluorescence intensity. In contrast, the majority of the dyes in latex particles are buried in a solid matrix. The encapsulated fluorophore was a doubly negatively charged carboxy derivative of fluorescein. The multiple charge significantly reduces the partition coefficient of carboxyfluorescein in the hydrophobic bilayer and hence its rate of leakage from a liposome.[24] By increasing the concentration of entrapped dye, it is possible to get more dye molecules per liposome, but the fluorescence signal per liposome (or the fluorescence yield) decreases because of the concentration quenching of dyes. Fluorescein, like other xanthene dyes, undergoes concentration quenching at high concentrations reducing the fluorescence yield.[25] The total number of fluorescein molecules in a liposome is ~219 000 but based on absorbance measurements (corrected for scattering), it was estimated that the number of unquenched fluorescein equivalents per liposome was ~79 500. In other words, the fluorescence yield of a liposome is 36%.

Figure 3 shows the size distribution of liposomes obtained from quasi-elastic light scattering measurements. Liposomes have an extremely narrow size distribution, which allows them to have uniform transport properties such as diffusion coefficient. Preparation of liposomes by an extrusion method provides a reproducible control over the size of liposomes, especially in the 50−500-nm range. Liposomes are also neutrally buoyant in water thus imparting minimal sedimentation velocity. More than 92 vol % of a liposome is occupied by water. Only the thin bilayer of lipids, typically 4 nm in thickness, makes liposomes slightly denser than water.

One of the most important requirements for particles to be useful in PIV is the stability of the suspension−particles should not aggregate over time. In a colloidal system, particles tend to aggregate due to various interactions, most notably hydrophobic
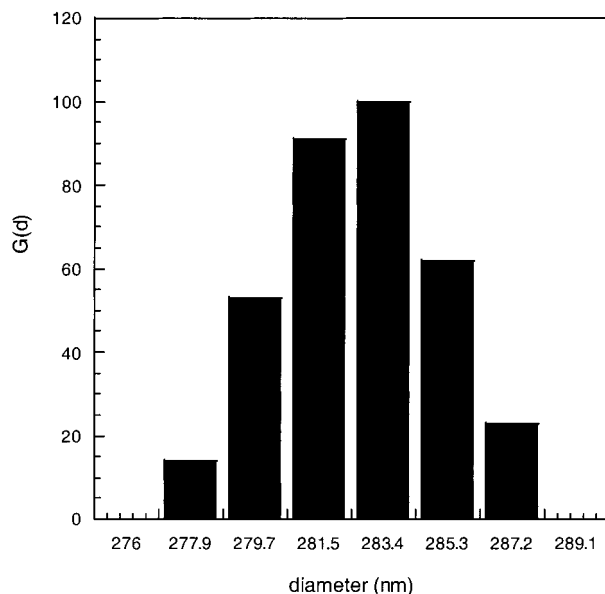
and van der Waals attractions. Electrostatic repulsion of surface charges is typically the stabilizing factor in a colloidal suspension. Since most of microfabricated structures are made in glass or silica, which are negatively charged at neutral pH, we synthesized liposomes that were negatively charged. Fluorescein-DHPE carries a −1 charge at neutral pH and hence their inclusion in the bilayer at 5 mol % accomplished two tasks: making the bilayer fluorescent and enhancing the net negative surface charge of the liposomes. The liposomes had a ζ potential of −58 mV at pH 7.0 in a 10 mM KCl solution. These liposomes showed no significant aggregation over six months and did not adsorb to silica (or glass) surfaces.

Figure 4a shows a raw fluorescence image of liposomes in an offset-cross junction of ~80−μm-wide rectangular microchannels. The liposomes appear as bright point sources of light that are randomly distributed through the channels. This image is drawn from a sequence of 300 images used to measure the depth-averaged velocity in the junction. This form of crossing junction can be used to inject a sample of controlled length into an electrophoretic separation channel. A common source of dispersion in these separations is unwanted pressure-driven flow produced by slight height or surface tension differences in liquid reservoirs that feed the separation system. The details of the velocity field near the junction are of interest in understanding the role of pressure-driven flow in sample dispersion during injection. The image sequence was taken of pressure-driven flow produced by small (<1 mm) differences in the fluid levels in the reservoirs. This sequence was processed to obtain the depth-averaged velocity field throughout the channels. Figure 4b shows the details of the velocity field in the upper left and lower right junctions. The maximum depth-averaged flow speed is ~50 μm/s. The flow at the channel boundaries does not slip, so the velocity drops to zero at the channel edges and the top and bottom surfaces. Because the channels are ~8 times wider than they are deep, gradients in the depth-wise direction are significantly larger than gradients across the image except in a narrow boundary layer near the edges of the channel. The extent of this boundary layer

(24) Fietchner, M.; Wong, M.; Bieniarz, C.; Shipchandler, M. T. *Anal. Biochem.* **1989**, *180*, 140−146.
(25) Chen, R. F.; Knutson, J. R. *Anal. Biochem.* **1988**, *172*, 61−78.
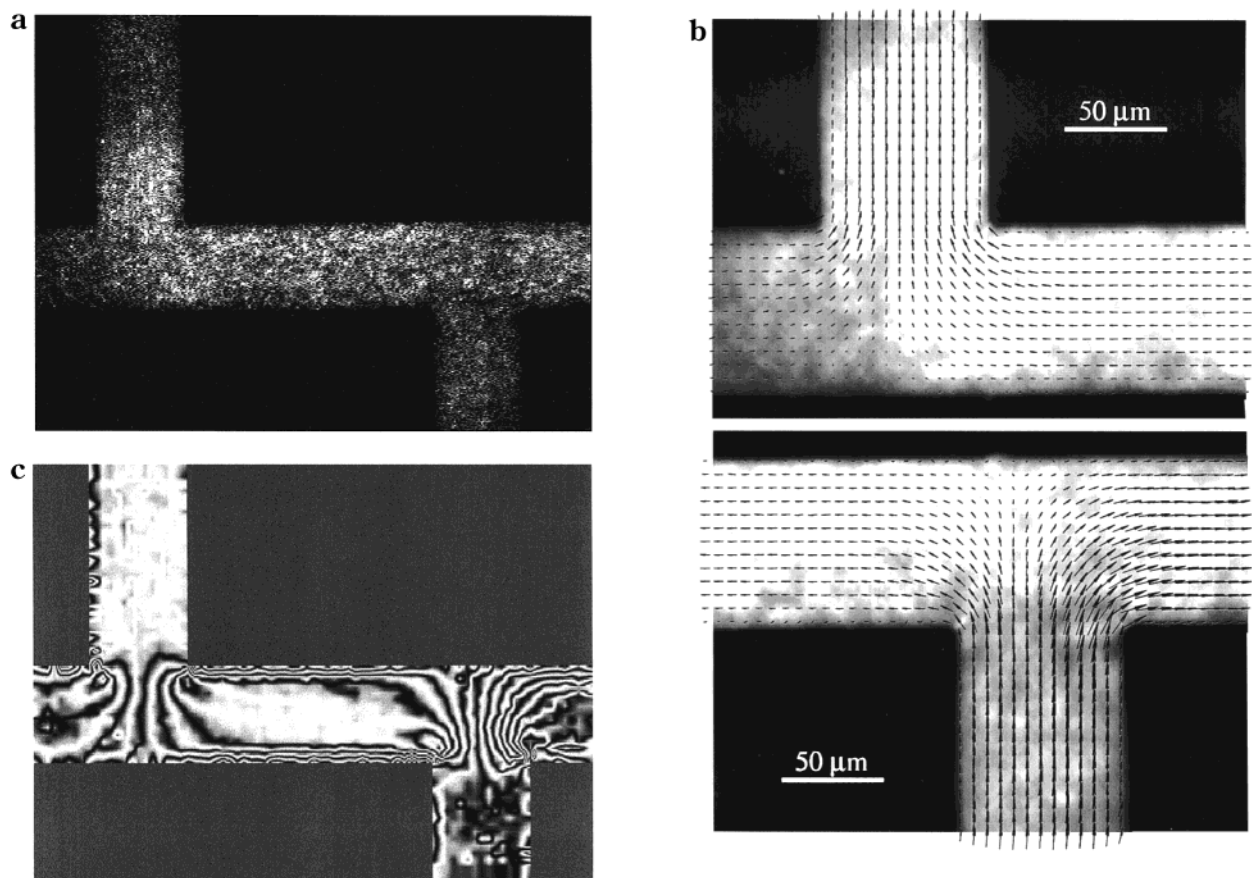
Figure 4. (a) Fluorescence image of a suspension of liposomes in an offset crossing junction. The field of view is 520 μm by 390 μm. (b) Overlay of measured velocity vectors and time-averaged fluorescence image of the flow in the upper left (top) and lower right (bottom) legs of the offset cross. (c) Contours of the mean flow velocity component in the left-to-right direction. The contour spacing is 0.5 pixels/frame or 12 μm/s. The unevenness of these contours reveals the velocity measurement uncertainty ($\sim$1−2 μm/s).

is approximately equal to the depth of the channels, consistent with the theory of Hele−Shaw flow and the theory of pressure-driven flow in a rectangular pipe. Figure 4c shows contours of the left-to-right components of the velocity field. These contours are spaced at 0.5 pixel/frame ($\sim$12 μm/s). The degree to which these contours do not vary smoothly is an indication of the uncertainty and scatter in the velocity measurement. Over much of the flow, the field is smooth to $\sim$0.1 fringe, corresponding to a $\sim$14 nm/frame particle displacement uncertainty, or 1.2 μm/s velocity uncertainty.

CONCLUSIONS

We have demonstrated the novel use of fluorescent liposomes as flow markers in a microscale PIV system. Liposomes have several advantages over the latex microspheres traditionally used for microscale PIV. They are neutrally buoyant in water, are hydrophilic, and carry a large number of fluorophores (up to 80 000 fluorescein equivalents) to provide a good S/N ratio. These liposomes are easy to synthesize from a large number of synthetic and natural lipids that allows them to be customized with respect to size, charge, and surface groups. Their easy disruption by surfactants or organic solvents allows for complete and easy removal from microfabricated structures. One limitation of liposomes is that their disruption in surfactant solutions or organic solvents excludes their use in applications where carrier liquid contains surfactants or solvents.